

Implications of O-X mode interference on large HF receive arrays

G.J. Frazer, T.J. Harris

ISRD, Defence Science and Technology Organisation, Edinburgh, SA 5111, AUSTRALIA

Abstract

High time resolution radar observations were made of the angle-of-arrival, power, group-delay and Doppler characteristics of oblique HF propagation at fixed frequencies, over a 1850km path in the north of Australia, during a 24-hour period in April 2004. It was observed that when the ordinary (O) and extra-ordinary (X) propagation modes in the F2 low ray were not separable, the expected amplitude fading occurred. Along with the energy fading, apparent elevation and azimuthal deviations were also observed indicating that the spatial structure of the received signal is distorted and non-planar. By increasing the effective Doppler and range resolutions the O and X modes are resolved and all of these “interference” effects were removed. It is concluded that interaction between unresolved O and X components in a given propagation path will cause received energy and angle-of-arrival to fluctuate on the tens of seconds time scale. When O and X components are resolved this fluctuation does not occur. The results shown, although measured by a comparatively small array (<100m per arm for a "L" array) imply that for the case of a large array, unless the received signal propagation paths are resolved into O and X components, there is likely to be at least one fade located somewhere spatially within the large array. This will distort the spatial signature of the received signal and may render spatial processing algorithms, such as classical beamforming and various adaptive spatial processing algorithms, ineffective. These algorithms are generally based on assumptions of a plane-wave, or set of plane-waves, impinging on the array. Polarimetric antenna elements can be used to separate O and X components in each propagation path. It is widely accepted that a polarimetric array can be used to ameliorate energy fading and in the case of HF radar can be used to improve target radar cross section properties. The result presented here suggests a third motivation for the use of a polarimetric array; that of preserving the spatial structure of the received signal for the case of very large receiving arrays. This may be crucial and as such can not be ignored in the design of large HF receiving systems, such as used in HF radar or radio astronomy. Mostly, in these cases, the prime purpose of the large array is to estimate, with high resolution, the spatial structure of received signals; or, to use the inherent spatial processing capability of the large array to improve the signal to noise ratio of a desired signal. In either case, we believe that spatial distortion of a skywave propagated signal will occur with increasing likelihood as the size of the receiving aperture increases and may in fact place an upper bound on the effective aperture of large HF arrays. This limitation may be removed using an array containing polarimetric elements.

Introduction

In April of 2004 DSTO conducted an HF propagation experiment using a 2-dimensional receive aperture in the Darwin region (Figure 1, 2 and 3). As part of this experiment transmissions were received from the Jindalee Over-the-Horizon Radar Network (JORN) transmitter site near Longreach (see Figures 1 and 4), 1850 km in range at a bearing of 133° True (129° Magnetic) from the receiver at Darwin. More information about the JORN is available in Cameron, 1995.

Figure 2 shows the receiver site layout including the locations of the antenna elements. GPS position coordinates for the key site items are shown on the drawing. The antenna array has 18 elements with an 8m spacing formed into an “L” shape to allow azimuth and elevation discrimination. The two end elements are passive and used to homogenise the mutual coupling within the array, the remaining 16 elements are connected to 16 digital receivers. Figure 3 is an aerial photograph of the receive array while Figure 4 shows the transmitter array.

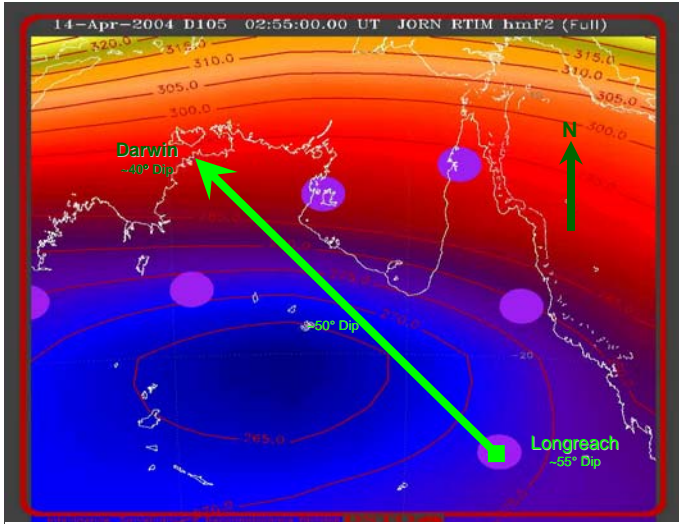


Figure 1 The path geometry showing the direct path from the transmitter to the receiver. The coloured contours indicate the ionospheric height at 0300 UT (near local noon at the midpoint of the path). Magenta circles are ionospheric sensor points used in generating the model ionosphere.

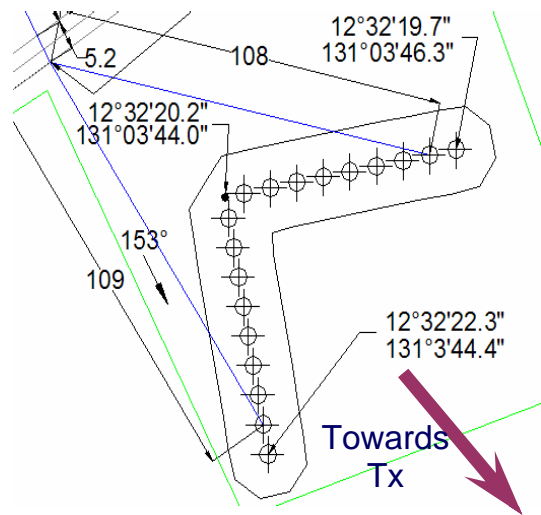


Figure 2 Location, orientation and dimensions of the receive array and control hut. Units are metres. The arms of the array are the same length

Data collection consisted of 9 sets of 30-minutes each of continuous digital samples over the period of 0304 to 2323 hours UT on 14th April 2004. Local time at the midpoint is approximately 10 hours ahead of UT. For each 30-minute period a fixed transmission frequency was used based on the propagation at the time. The one-way path transmission was a coherent radar waveform. This waveform allowed the generation of a “channel-scatter-function” (CSF) as a function of time. The CSF shows the propagated energy as a function of Doppler and time delay. This information is useful for describing the state of the ionosphere and its effects on HF signals [e.g. Basler *et al* 1988, Angling *et al* 1998].

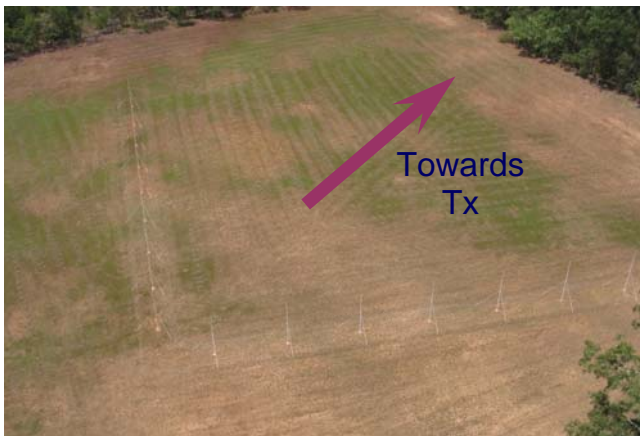


Figure 3. Aerial view of the receiver array



Figure 4. View of the transmitter array at Longreach.

Results

Short Period Integrations

A CSF was generated every 2 seconds (see Figure 5) using overlapped processing and a 6 second coherent integration time (CIT). When the CSF is formed, the received energy is binned into a range of Doppler velocities and time-of-flight. In this case, the Doppler velocity is displayed along the x-axis, converted to radial velocity with outbound speeds being positive, and time-of-flight, expressed as a group-range, is displayed along the y-axis. For every Doppler/group-range bin

there is an estimate of the received energy and an estimated angle-of-arrival based on the peak from beam-forming in elevation and azimuth. The energy (normalised to the F2 low-ray peak), elevation and azimuth for each Doppler x Group-range bin are displayed from left-to-right in Figure 5. Estimated peak positions are overlaid on each image. The two horizontal red lines on the left-most panel are automatically determined bounds for the energy returns from a F2 low-ray mode.

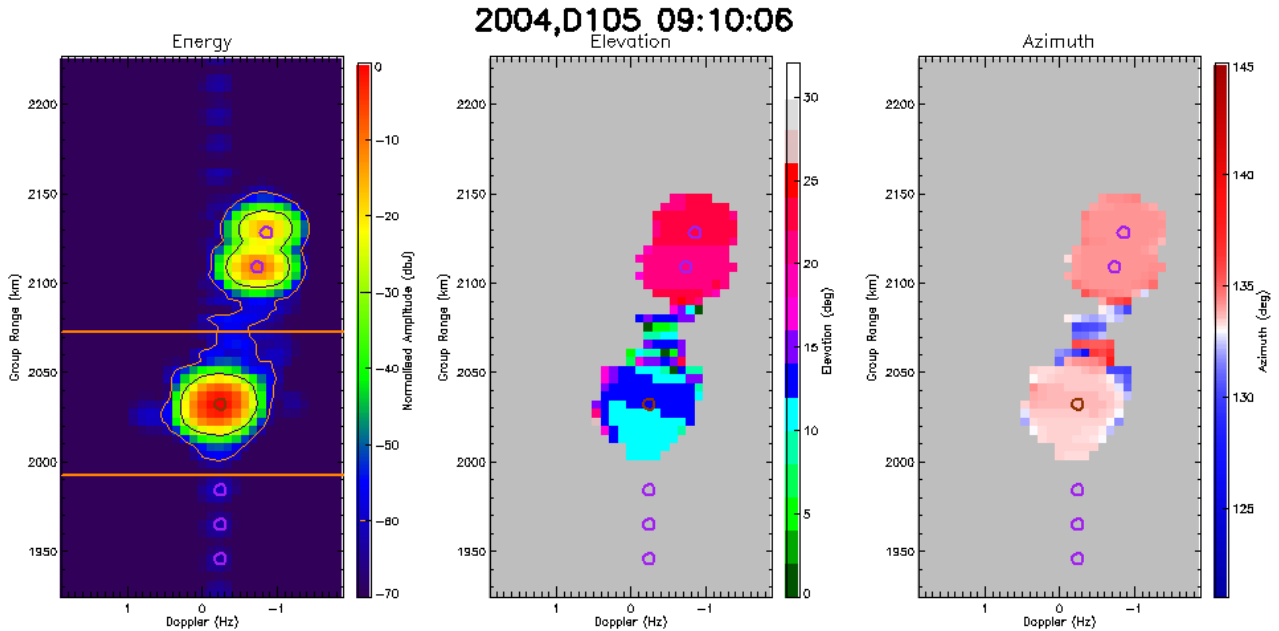


Figure 5. Channel scatter function with estimated peak positions overlaid. From left-to-right: the normalised energy, the elevation, and the azimuth for each Doppler x group-range bin. 6s CIT

As direction estimates are meaningless for low signal-to-noise ratios, an amplitude threshold has been applied. The threshold was chosen as a fixed level of 60dB down from the peak energy. Qualitatively this appeared to remove the noise but leave the signal. The contour lines in the left-most panel of Figure 5 are at -30 and -60 dB. The regions of the CSF display that fall below the threshold are shaded grey in the elevation and azimuth panels of the figure.

Analysis has shown that the elevation estimates, although consistent in relative values, are inaccurate in their absolute values at low elevations. This is due to poor discrimination at low elevations arising from the small array baseline and the antenna elevation patterns of the individual elements. The result is that low elevation estimates are biased high.

This paper shows a small segment of the full data set but this segment is typical. We consider that the results presented here are representative of the full data set.

Figure 6 displays the time evolution of the properties of the peaks in the CSF energy for a time period near local noon. Unresolved O/X returns in the F2 low trace cause amplitude fading of the order of 20-30dB, with a period of the order of one cycle per minute.

Each fade in the F2 low energy is associated with an apparent abrupt change in the detected azimuth and elevation of the peak. Closer inspection of the spectral shape shows that a broadening of both the elevation and azimuthal distributions of the peak is also associated with the fading events. The direct-path energy becomes more widely distributed in solid angle as the O and X components interfere.

Another feature evident in the temporal evolution of the peaks is the stability of the F2 high-ray signal in direction-of-arrival and in energy. At the frequency being used the O and X components are resolved in Doppler/group-range for the high-ray, removing what appears to be the major cause of the directional and energy variability in the F2 low-ray peaks.

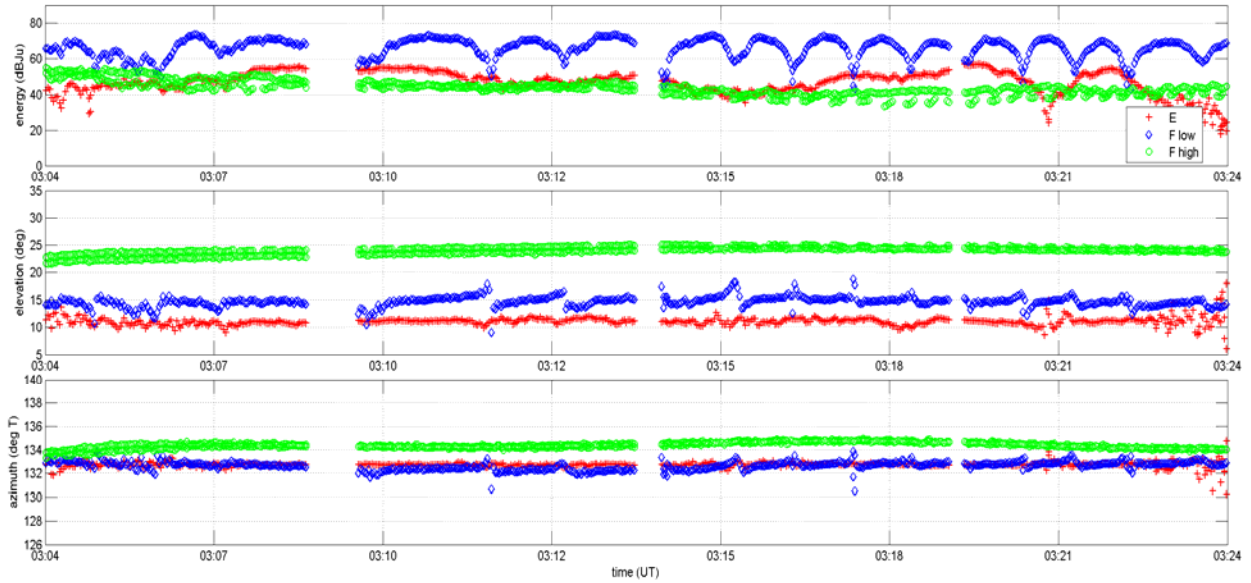


Figure 6. Temporal properties of the energy peaks in the CSF data.

Long period integrations

In order to verify that the observed fading and spatial distortion in the wave front are due to the interaction of the unresolved O and X modes the data was reprocessed with a longer coherent integration time of 120 seconds. An example of the resultant channel scatter function is shown in Figure 7

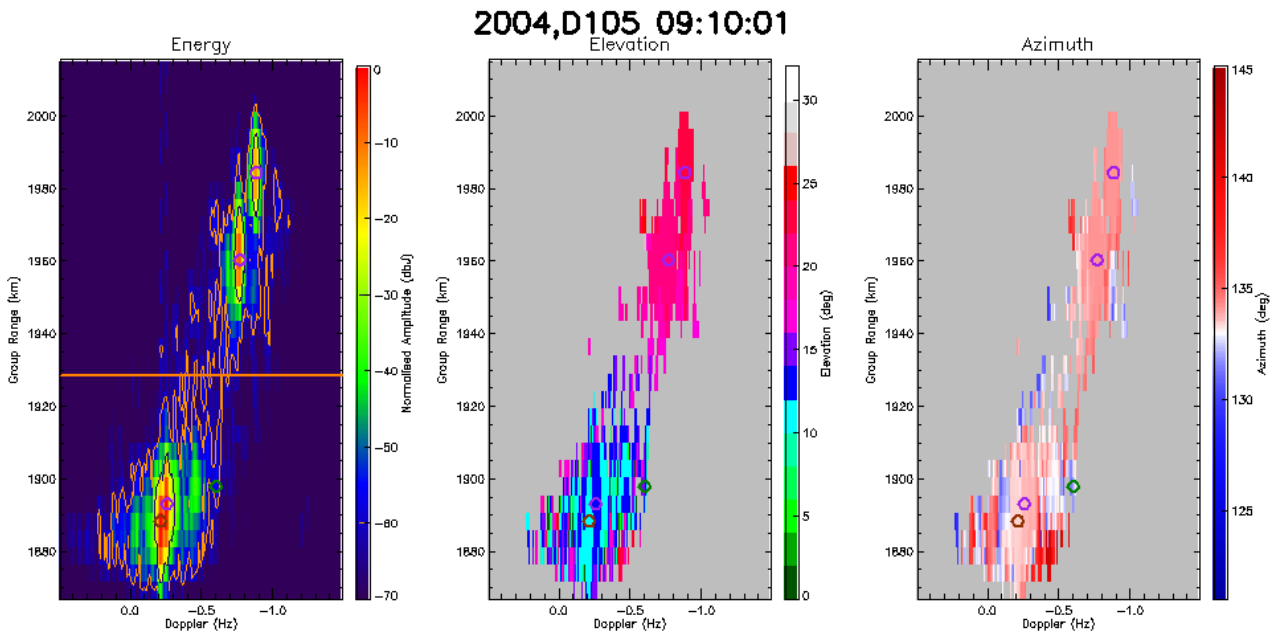


Figure 7. Channel scatter function with estimated peak positions overlaid. From left-to-right: the normalised energy, the elevation, and the azimuth for each Doppler x group-range bin. 120 s CIT. Note O-X separation for both the F2-low and F2-high rays.

Figure 8 displays the characteristics of the energy peaks for the four minute period from 0909 to 0913. The left-hand set of panels show the results for the 6 second CIT while the right-hand set of panels show the results for the longer, 120 second, CIT. The same features as discussed for Figure 6 are apparent for the shorter CIT dataset although the dominant fading rate has increased. The unresolved O/X modes of the F2-low ray cause amplitude fading and a distorted and variable spatial

structure for the signal wave front while the resolved O and X modes of the F2-high rays show stable amplitude and a plane-wave spatial structure. The longer CIT has resolved the O and X modes for both the F2-high and low rays, removing the amplitude fading and regularizing the wave front spatial structure.

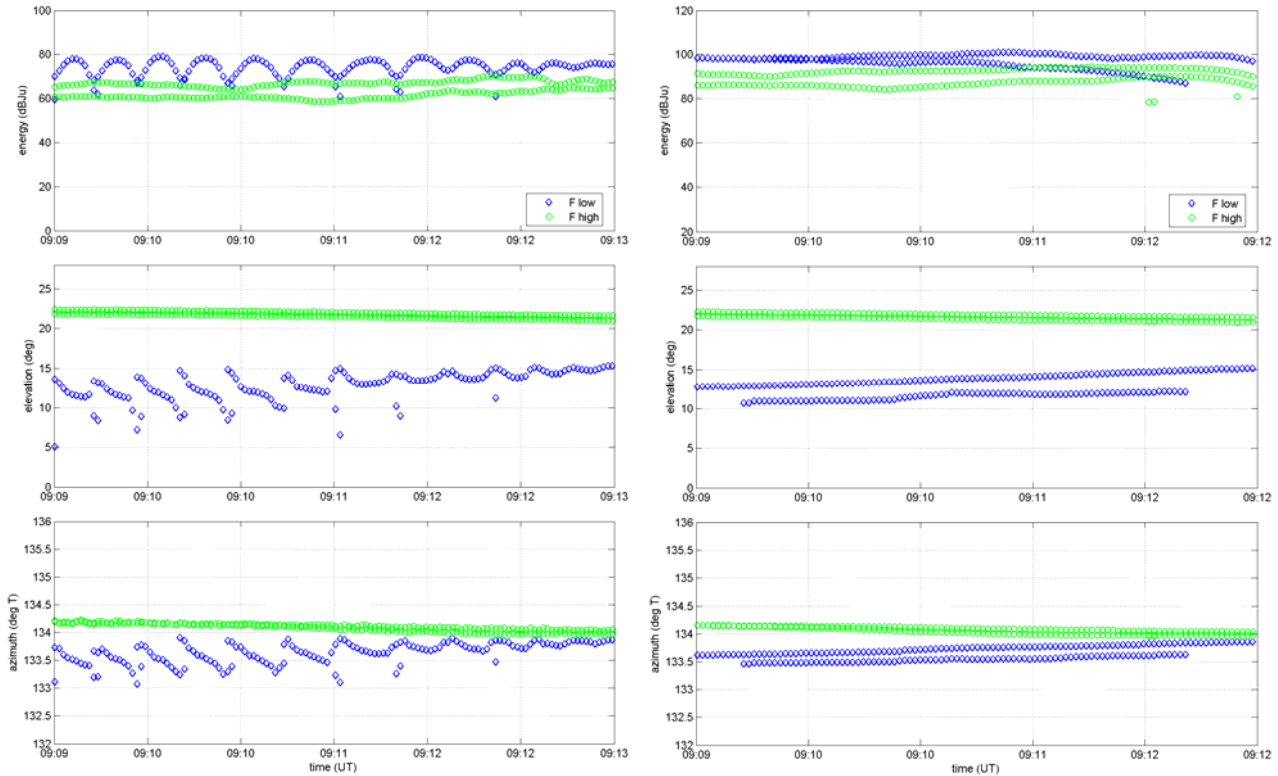


Figure 8. Temporal properties of the energy peaks in the CSF data from 0909 to 0913 UT for day 105 of 2004. From top to bottom are shown the time-series of the amplitude, elevation and azimuthal variations respectively. The left-hand column shows the results of unresolved O-X modes on the F2-low path (6s CIT) while the right-hand column shows the same data processed to resolve the O-X F2-low rays (120s CIT)

Conclusions

It is concluded that interaction between unresolved O and X components in a given propagation path will cause the received energy and angle-of-arrival to fluctuate on the tens of seconds time scale. When O and X components are resolved this fluctuation does not occur. The results shown, were measured by a comparatively small array (<100m per arm for a "L" array). One can also postulate that the behaviour observed for a very large receiving aperture, but at a single CIT, will show similar behaviour. This implies that for a larger array, unless the received signal propagation paths are resolved into O and X components, there is likely to be at least one fade located somewhere spatially within the large array. This will distort the spatial structure of the received signal and may render spatial processing algorithms, such as classical beamforming and various adaptive spatial processing algorithms, ineffective. These algorithms are generally based on assumptions of a plane-wave, or set of plane-waves, impinging on the array.

Polarimetric antenna elements can be used to separate O and X components in each propagation path. It is widely accepted that a polarimetric array can be used to ameliorate energy fading and in the case of HF radar can be used to improve target radar cross section properties [see for example Anderson *et al* 2000 and the references contained therein].

The result presented here suggests a third motivation for the use of a polarimetric array; that of preserving the spatial structure of the received signal for the case of very large receiving arrays. This may be crucial and as such can not be ignored in the design of large HF receiving systems, such as used in HF radar or radio astronomy. Mostly, in these cases, the prime purpose of the large array is to estimate, with high resolution, the spatial structure of received signals; or, to use the inherent spatial processing capability of the large array to improve the signal to noise ratio of a desired signal. In either case, we believe that spatial distortion of a skywave propagated signal will occur with increasing likelihood as the size of the receiving aperture increases and may in fact place an upper bound on the effective aperture of large HF arrays. This limitation may be removed using an array containing polarimetric elements.

References

- Anderson, S.J., Y.I. Abramovich, (2000). Recent developments in HF skywave radar polarimetry, *Proceedings of IEEE Geoscience and Remote Sensing Symposium, 2000*, **3**, 1319-1322, 2000.
- Angling, M. J., P. S. Cannon, N. C. Davies, T. J. Willink, V. Jodalen, and B. Lundborg (1998). Measurements of Doppler and multipath spread on oblique high-latitude HF paths and their use in characterizing data modems, *Radio Sci.*, **33**, 97-107, 1998.
- Basler, R. P., G. H. Price, R. T. Tsunoda, and T. L. Wong, (1988). Ionospheric distortion of HF signals, *Radio Sci.*, **23**, 569-579, 1988.
- Cameron, A. (1995). The Jindalee operational radar network: its architecture and surveillance capability. *Record of the IEEE 1995 International Radar Conference*, 692-697, 1995.